

Cubes, Squares, and Books: A Simple Transition Metal/Bridging Ligand Combination Can Lead to a Surprising Range of Structural Types with the Same Metal/Ligand Proportions

Adel M. Najar, Ian S. Tidmarsh, Harry Adams, and Michael D. Ward*

Department of Chemistry, University of Sheffield, Sheffield S3 7HF, U.K.

Received September 24, 2009

Reaction of two structurally related bridging ligands L^{26Py} and L^{13Ph} , in which two bidentate chelating pyrazolyl-pyridine units are connected to either a 2,6-pyridine-diyl or 1,3-benzene-diyl central group via methylene spacers, with first-row transition metal dications, results in a surprising variety of structures. The commonest is that of an octanuclear coordination cage $[M_8L_{12}]X_{16}$ [$M = Co(II)$ or $Zn(II)$; $X = perchlorate$ or tetrafluoroborate] in which a metal ion is located at each of the eight vertices of an approximate cube, and one bis-bidentate bridging ligand spans each edge. The arrangement of *fac* and *mer* tris-chelate metal centers around the inversion center results in approximate (non-crystallographic) S_6 symmetry. Another structural type observed in the solid state is a hexanuclear complex $[Co_6(L^{13Ph})_9](ClO_4)_{12}$ in which the six metal ions are in a rectangular array (two rows of three), folded about the central Co–Co vector like a partially open book, with each metal–metal edge containing one bridging ligand apart from the two outermost metal–metal edges which are spanned by a pair of bridging ligands in a double helical array. The final structural type we observed is a tetranuclear square $[Ni_4(L^{26Py})_6](BF_4)_8$, with the four Ni–Ni edges spanned alternately by one and two bridging ligand such that it effectively consists of two dinuclear double helicates cross-linked by additional bridging ligands. A balance between the “cube” and “book” forms, which varied from compound to compound, was observed in solution in many cases by 1H NMR and ES mass spectrometry studies.

Introduction

We¹ and many others² are investigating the self-assembly, structural properties, and host–guest chemistry of hollow metal complex cages. Such cages can have elaborate polyhedral shapes of striking complexity which form from very simple component parts,^{1,2a,f} and the constrained, often hydrophobic environment inside the cages allows the cavities to accommodate and stabilize reactive guest species which would otherwise be short-lived, and change the course of a chemical reaction.²ⁱ Recent elegant examples of this include the stabilization of a molecule of white phosphorus inside the tetrahedral cavity of an M_4L_6 cage,³ and the huge

acceleration of an aza-Cope rearrangement inside a cage cavity.⁴

The structures of such polyhedral cages arise from a balance of many factors. With the bis-bidentate ligands that we have used containing two bidentate pyrazolyl-pyridine binding sites,¹ the most obvious is the stoichiometric issue associated with combining six-coordinate metal ions with ligands containing four donor atoms. To ensure that all metal ions are coordinatively saturated, and all ligands use all of their binding sites, a ratio of 1.5 ligands per metal ion is needed which results in a 2:3 M/L ratio.¹ This principle has been expressed by different researchers as “principle of maximum site occupancy”⁵ or “avoidance of valence frustration”.⁶ This 2:3 metal/ligand ratio can be expressed in numerous different ways, ranging from M_4L_6 tetrahedra, the smallest cages that have a well-defined interior cavity, to $M_{16}L_{24}$ capped truncated tetrahedra whose large cavity accommodates eight counterions and some solvent molecules.¹ An additional driving force that influences the

*To whom correspondence should be addressed. E-mail: m.d.ward@sheffield.ac.uk.

(1) Ward, M. D. *Chem. Commun.* **2009**, 4487 and refs therein.
(2) Reviews on coordination cages: (a) Swiegers, G. F.; Malefetse, T. J. *Coord. Chem. Rev.* **2002**, 225, 91. (b) Fujita, M.; Tominaga, M.; Hori, A.; Therrien, B. *Acc. Chem. Res.* **2005**, 38, 369. (c) Fiedler, D.; Leung, D. H.; Bergman, R. G.; Raymond, K. N. *Acc. Chem. Res.* **2005**, 38, 349. (d) Hamilton, T. D.; MacGillivray, L. R. *Cryst. Growth Des.* **2004**, 4, 419. (e) Garay, A. L.; Pichon, A.; James, S. L. *Chem. Soc. Rev.* **2007**, 36, 846. (f) Alvarez, S. *Dalton Trans.* **2006**, 2209. (g) Saalfrank, R. W.; Uller, E.; Demleitner, B.; Bernt, I. *Struct. Bonding (Berlin)* **2000**, 96, 149. (h) Stang, P. J.; Seidel, S. R. *Acc. Chem. Res.* **2002**, 35, 972. (i) Yoshizawa, M.; Klosterman, J. K.; Fujita, M. *Angew. Chem. Int. Ed.* **2009**, 48, 3418.

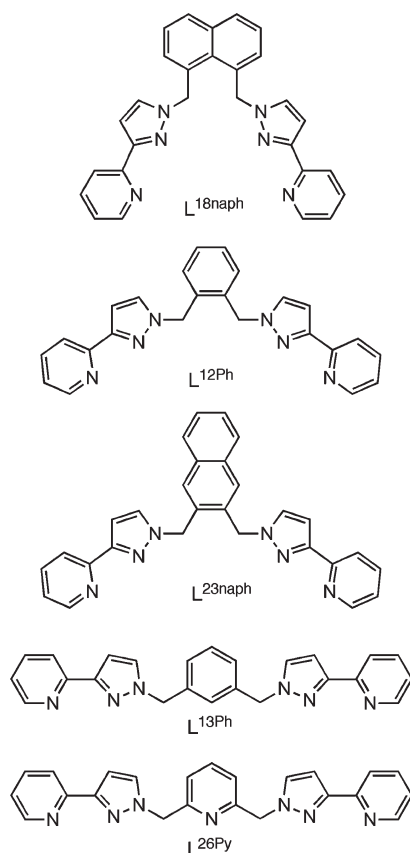
(3) Mal, P.; Breiner, B.; Rissanen, K.; Nitschke, J. R. *Science* **2009**, 324, 1697.

(4) Hastings, C. J.; Fiedler, D.; Bergman, R. G.; Raymond, K. N. *J. Am. Chem. Soc.* **2008**, 130, 10977.

(5) Kramer, R.; Lehn, J.-M.; Marquis-Rigault, A. *Proc. Natl. Acad. Sci. U.S.A.* **1993**, 90, 5394.

(6) Hutin, M.; Bernardinelli, G.; Nitschke, J. R. *Proc. Natl. Acad. Sci. U.S.A.* **2006**, 103, 17655.

Scheme 1



structures of the cages is the aromatic π -stacking between electron-rich and electron-poor fragments of different ligands which is extensive in many of the structures and appears to contribute substantially to solution stability.¹

In most cases studied so far a given ligand will generate the same polyhedral cage structure with a range of different (but similar) M^{2+} cations. Thus, for example, L^{18naph} (Scheme 1) reacts with Cu(II), Co(II), and Cd(II) salts to afford isostructural $[M_{12}L_{18}]^{24+}$ truncated tetrahedral cages despite the modest differences in ionic radius and the preference of Cu(II) for a less regular coordination geometry.⁷ In contrast however, L^{12Ph} and L^{23naph} afford only $[M_4L_6]^{8+}$ tetrahedral cages with Co(II) and Zn(II),⁸ but give the simpler dinuclear complex $[Ni_2L_3]^{4+}$ with Ni(II) which contains two terminal tetradentate and one bis-bidentate bridging ligand, that is, $[LNi-(\mu-L)-NiL]^{4+}$, with no evidence for formation of a tetrahedral cage.^{8a,b} We ascribed this to the slightly smaller ionic radius of Ni(II) compared to Co(II) and Zn(II) in octahedral geometry which would result in increased steric strain in the tightly packed cage assembly that could be alleviated by adoption of a more open structure.

In this paper we describe the coordination behavior of the related pair of ligands L^{26Py} and L^{13Ph} which, on reaction

with labile first row transition metal ions, generates either octanuclear M_8L_{12} cages with an approximately cubic topology or simpler M_4L_6 or M_6L_9 assemblies with hitherto unknown (in this series) structures that are based on interconnected double helical fragments. In all cases the 2:3 M/L ratio is maintained but now we observe in the solid state three different structural types, two of which arise from the *same* metal and ligand combination and therefore appear to be of very similar energy. The same “instructions” for the self-assembly process can therefore lead to two quite different outputs. We report here the synthesis and structural characterization of a series of complexes, plus solution NMR and mass spectrometric studies which reveal some surprising differences between the solid state and solution behavior of the compounds. A variety of groups have reported cubic coordination cages prepared using a range of different self-assembly strategies.

Preliminary accounts of some of this work have been published in two earlier communications, including the crystal structures of $[Zn_8(L^{13Ph})_{12}](BF_4)_{16}$, $[Zn_8(L^{26Py})_{12}](ClO_4)_{16}$, and $[Co_6(L^{13Ph})_9](ClO_4)_{12}$.¹⁰

Results and Discussion

Ligand Syntheses. The ligands used, L^{26Py} and L^{13Ph} , are shown in Scheme 1; they were prepared by reaction of 3-(2-pyrazol-1-yl)pyridine with 2,6-bis(bromomethyl)pyridine or 1,3-bis(bromomethyl)benzene, respectively, in the usual way under basic conditions.¹⁰ L^{13Ph} is of course tetradentate with two bidentate chelating sites; L^{26Py} may act as a pentadentate ligand if the central pyridyl ring also becomes involved in coordination.

Structures of Octanuclear Cubic Complexes with Co(II) and Zn(II). Reaction of either of these ligands with Co(II) or Zn(II) salts (perchlorate or tetrafluoroborate) in a 2:3 M/L ratio in MeOH as solvent afforded solid products which, after recrystallization, afforded crystals of octanuclear cubic cages of general formula $[M_8L_{12}]X_{16}$. We have structurally characterized the following five examples of these: $[Zn_8(L^{13Ph})_{12}](BF_4)_{16}$; $[Zn_8(L^{13Ph})_{12}](ClO_4)_{16}$; $[Co_8(L^{13Ph})_{12}](BF_4)_{16}$; $[Zn_8(L^{26Py})_{12}](ClO_4)_{16}$; and $[Co_8(L^{26Py})_{12}](BF_4)_{16}$.

These all have the same general structure, with minor but significant differences; we use the structure of $[Co_8(L^{13Ph})_{12}](BF_4)_{16}$ here as an illustration (Figures 1 and 2). The eight Co(II) ions are arrayed at the corners of an approximate cube, with a bridging ligand L^{13Ph} spanning each of the twelve edges (Figure 1). The presence of eight vertices (metal ions) and twelve edges (bridging

(7) (a) Bell, Z. R.; Jeffery, J. C.; McCleverty, J. A.; Ward, M. D. *Angew. Chem., Int. Ed. Engl.* **2002**, *41*, 2515. (b) Argent, S. P.; Adams, H.; Riis-Johannessen, T.; Jeffery, J. C.; Harding, L. P.; Mamula, O.; Ward, M. D. *Inorg. Chem.* **2006**, *45*, 3905.

(8) (a) Fleming, J. S.; Mann, K. L. V.; Carraz, C.-A.; Psillakis, E.; Jeffery, J. C.; McCleverty, J. A.; Ward, M. D. *Angew. Chem., Int. Ed. Engl.* **1998**, *37*, 1279. (b) Paul, R. L.; Bell, Z. R.; Jeffery, J. C.; McCleverty, J. A.; Ward, M. D. *Proc. Natl. Acad. Sci. U.S.A.* **2002**, *99*, 4883. (c) Tidmarsh, I. S.; Taylor, B. F.; Hardie, M. J.; Russo, L.; Clegg, W.; Ward, M. D. *New J. Chem.* **2009**, *33*, 366.

(9) (a) Suzuki, K.; Tominaga, M.; Kawano, M.; Fujita, M. *Chem. Commun.* **2009**, 1638. (b) Cao, M. L.; Hao, H.-G.; Zhang, W.-X.; Ye, B. H. *Inorg. Chem.* **2008**, *47*, 8126. (c) Abrahams, B. F.; Egan, B. F.; Robson, R. *J. Am. Chem. Soc.* **1999**, *121*, 3535. (d) Roche, S.; Haslam, C.; Adams, H.; Heath, S. L.; Thomas, J. A. *Chem. Commun.* **1998**, 1681. (e) Klausmeyer, K. K.; Wilson, S. R.; Rauchfuss, T. B. *J. Am. Chem. Soc.* **1999**, *121*, 2705. (f) Zimmer, A.; Kuppert, D.; Weyhermüller, T.; Müller, I.; Hegetschweiler, K. *Chem.—Eur. J.* **2001**, *7*, 917. (g) Lang, J.-P.; Xu, Q.-F.; Chen, Z.-N.; Abrahams, B. F. *J. Am. Chem. Soc.* **2003**, *125*, 12682. (h) Schelter, E. J.; Prosvirin, A. V.; Dunbar, K. R. *J. Am. Chem. Soc.* **2004**, *126*, 15004. (i) Liu, Y.; Kravtsov, V.; Walsh, R. D.; Poddar, P.; Srikanth, H.; Eddaoudi, M. *Chem. Commun.* **2004**, 2806. (j) Cheng, A.-L.; Liu, N.; Zhang, J.-Y.; Gao, E.-Q. *Inorg. Chem.* **2007**, *46*, 1034. (k) Heinrich, J. L.; Berseth, P. A.; Long, J. R. *Chem. Commun.* **1998**, 1231.

(10) (a) Bell, Z. R.; Harding, L. P.; Ward, M. D. *Chem. Commun.* **2003**, 2432. (b) Argent, S. P.; Adams, H.; Harding, L. P.; Ward, M. D. *Dalton Trans.* **2006**, 542.

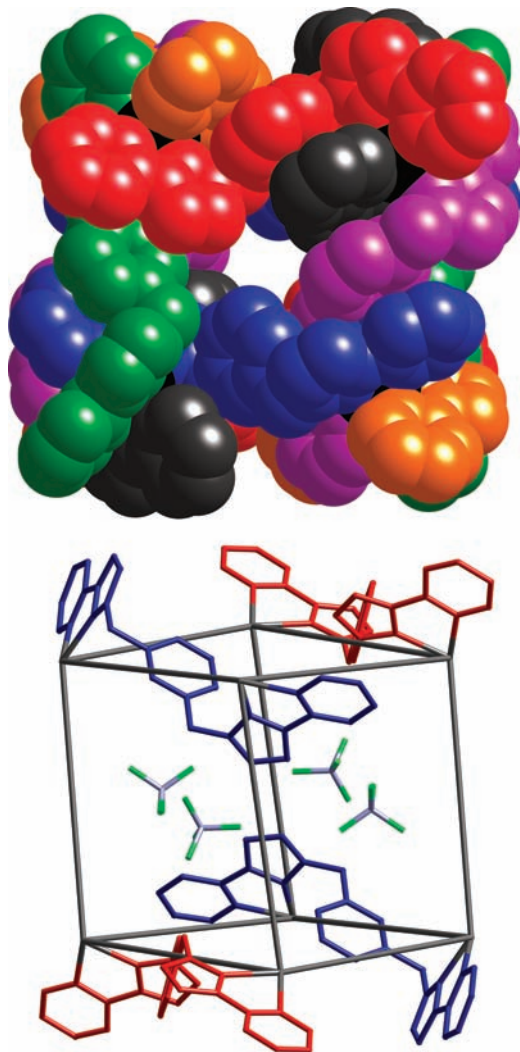


Figure 1. Two views of the structure of the cubic cage complex cation of $[\text{Co}_8(\text{L}^{13\text{Ph}})_{12}(\text{BF}_4)_{16}]$. Top: a space-filling picture. Bottom: a view containing only four of the twelve bridging ligands, with the anions lying inside the central cavity also shown. Crystallographically equivalent ligands are colored the same in each case.

ligands) in a cube neatly matches the requirements of the “maximum site occupancy” principle, thereby allowing the required 2:3 M/L ratio to be adopted. Each metal ion, being at the conjunction of three edges of the cube, therefore interacts with a bidentate chelating fragment from each of three different ligands to give the preferred 6-fold coordination. The separations between metal ions along the edges of the cube lie in the range 9.61 Å [Co(2)–Co(4)] to 10.60 Å [Co(1)–Co(2)], with the Co–Co–Co angles at the corners varying from 80.3° to 100.1°.

The pseudo-cubic structure has some interesting subtleties associated with it. The four independent Co(II) centers (the complex cation lies astride an inversion center in space group $P\bar{1}$) do not all have the same geometric configuration. Co(3) has a *fac* geometry associated with the three pyrazolyl-pyridine chelates, with all three 2-pyridyl ligands at the outermost part of the complex structure and all being *trans* to a pyrazolyl group. Obviously the diagonally opposite, symmetry-equivalent metal center Co(3A) likewise has a *fac* geometric configuration but is the opposite optical configuration. In

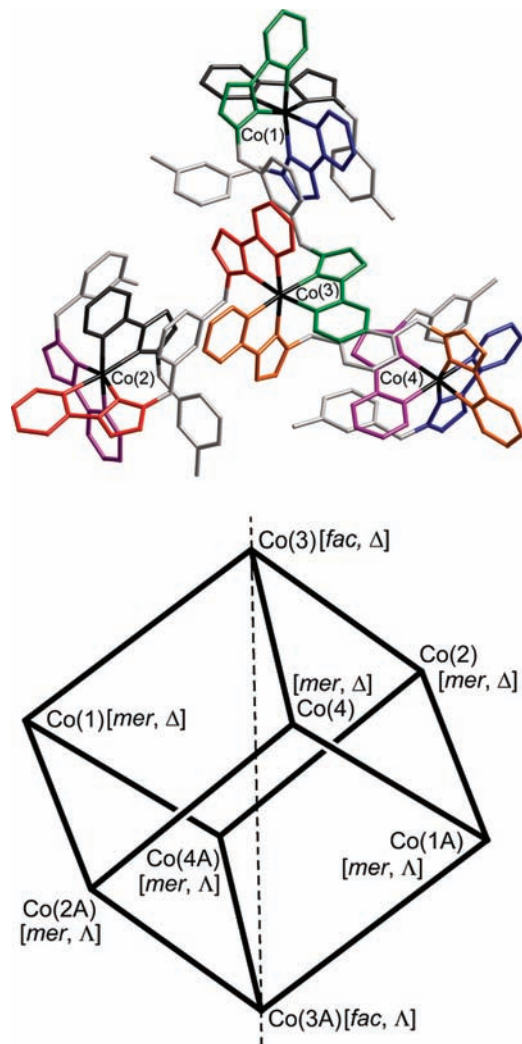


Figure 2. Additional partial views of the structure of $[\text{Co}_8(\text{L}^{13\text{Ph}})_{12}(\text{BF}_4)_{16}]$. Top: a view down the *pseudo*- C_3/S_6 axis [Co(3) has a *fac* tris-chelate arrangement; Co(1), Co(2), and Co(4) all have a *mer* tris-chelate arrangement]. Only the coordinated pyrazolyl-pyridine fragments are colored to emphasize them. Bottom: a sketch showing the overall symmetry of the cage cation with the C_3/S_6 axis shown as a dotted line.

contrast, the other metal centers all have a *mer* tris-chelate geometry in which one axis of the octahedron contains two pyridyl ligands, another contains two pyrazolyl ligands, and the third contains a pyridyl ligand *trans* to a pyrazolyl ligand. These three metal centers [Co(1), Co(2), and Co(4)] all have the same optical configuration as each other [and the same as the adjacent Co(3) in the same asymmetric unit]. Thus there is an approximate C_3 axis along the long diagonal of the cube from Co(3) to Co(3A), which is also an S_6 axis; we have seen this general structural type before in a different series of cubic cages based on a different bridging ligand.¹¹ The symmetry is illustrated in Figure 2.

The ligands are substantially folded at the methylene “hinge” positions, and this flexibility allows them to adopt an arrangement in which they are all involved in interligand aromatic π -stacking. Along each of the twelve edges of the

(11) Tidmarsh, I. S.; Faust, T. B.; Adams, H.; Harding, L. P.; Russo, L.; Clegg, W.; Ward, M. D. *J. Am. Chem. Soc.* **2008**, *130*, 15167.

cube, the central phenyl group from one ligand is sandwiched between coordinated pyrazolyl-pyridine groups of two others to give a π -stack of alternating electron deficient/electron rich/electron deficient aromatic units, with characteristic separations of about 3.5 Å between approximately parallel planes. The pyrazolyl-pyridine units are particularly electron deficient not only because of the number of N atoms in the rings, but because of their coordination to a 2+ metal center which means that they will carry a substantial residual positive charge. Such a donor/acceptor arrangement is known to lead to strong π -stacking¹² and is reminiscent of the dialkoxybenzene/viologen donor/acceptor stacks exploited extensively by Stoddart as a templating principle.¹³ We have seen this type of alternating donor/acceptor stacking in several of our series of polyhedral cages and it appears to make an important contribution to their formation and stability.¹

The final point to notice about the structure of the cage is the central cavity, which in this structure accommodates four $[\text{BF}_4]^-$ anions (Figure 1). These are not centrally located in the cavity but lie at the periphery of the central cavity, more associated with the windows in four of the square faces (the other two faces of the cube, an opposed pair, do not have anions associated with them in the same way). These four anions are quite close together, with B···B distances of 5.84 Å [B(11)···B(61)], and 6.26 Å [B(11)···B(61A)], which results in F···F separations of just 3.41 Å [F(12)···F(64)] and 3.72 Å [F(15)···F(65A)] between their peripheries.

In $[\text{Zn}_8(\text{L}^{13\text{Ph}})_{12}](\text{BF}_4)_{16}$ (reported in an earlier communication)^{10b} the cube is a little more regular with Zn···Zn separations in the range 9.72 to 10.27 Å. Zn(1) and its symmetry equivalent Zn(1A) are the two metal centers with a *fac* rather than a *mer* tris-chelate configuration, and this defines the *pseudo-S*₆ axis. There are two $[\text{BF}_4]^-$ anions lying clearly well within the central cavity, and an additional four a little further out that lie above the windows in four of the faces (Figure 3). Again some of the anion–anion contacts are short, with the B(10)···B(10A) separation between the two $[\text{BF}_4]^-$ anions within the cavity being 5.18 Å and the closest F···F contact between them being about 3.8 Å (the F atoms involved exhibit disorder so there is no point being more precise than this). The perchlorate analogue $[\text{Zn}_8(\text{L}^{13\text{Ph}})_{12}](\text{ClO}_4)_{16}$ is very similar (although not crystallographically isomorphous) with Zn···Zn separations of 9.51–10.16 Å and two perchlorate anions in the cavity on either side of an inversion center, again resulting in quite short O···O separations of 3.83 Å between anions. Zn(2) and Zn(2A) are the *fac* metal centers which define the *pseudo-S*₆ axis. Because of the similarity with the tetrafluoroborate salt a figure is not shown.

Somewhat surprisingly replacement of the central 1,3-disubstituted phenyl ring with a pyridine-2,6-diyl group, making the ligand potentially pentadentate, did not affect formation of cube structures: the central pyridyl ring does not participate in coordination to metal ions in the Co(II) and Zn(II) complexes such that $\text{L}^{26\text{Py}}$ coordinates in the same manner as $\text{L}^{13\text{Ph}}$, as a bis-bidentate bridging ligand. $[\text{Co}_8(\text{L}^{26\text{Py}})_{12}](\text{BF}_4)_{16}$ has the same type of structure as the

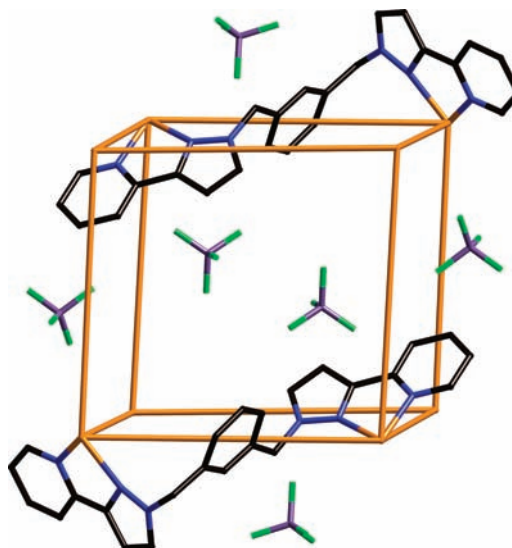


Figure 3. Partial view of the structure of the complex cation $[\text{Zn}_8(\text{L}^{13\text{Ph}})_{12}](\text{BF}_4)_{16}$, including only 2 of the 12 bridging ligands, showing 2 anions lying inside the cage cavity.

two complexes reported above and therefore does not need to be discussed in detail. The Co···Co separations along the edges of the cube lie in the range 9.75 to 10.17 Å, with Co(1) having the *fac* tris-chelate geometry and therefore the Co(1)—Co(1A) vector being the *pseudo-S*₆ axis. The cavity in this case contains one $[\text{BF}_4]^-$ anion at the exact center (with the F atoms disordered given the requirement for inversion symmetry) and an additional six plugging the gap in the center of each of the six faces of the cube (Figure 4a). The anion–anion distances are greater here, with B···B separations between the central anion and the six peripheral ones all being considerably greater than 7 Å. The N atoms of the central pyridyl rings on the bridging ligands are not obviously interacting with anything (for example, there is no evidence of them acting as H-bond acceptors to lattice water molecules). They are oriented in various directions with some of the N atom lone pairs pointing into the central cavity, some being approximately tangential, and some pointing outward (Figure 4b). The possibility that an array of 12 “free” pyridyl groups could orient their lone pairs toward the center, acting as a three-dimensional H-bond accepting array, is a tantalizing one but is not operative here. We note, however, that the presence of only one anion in the center of this cube, rather than two or four in the earlier examples, may be associated with the tendency of the anions to avoid those electron lone pairs from the pyridyl groups that are directed inward toward the center of the cubes.

The final example, $[\text{Zn}_8(\text{L}^{26\text{Py}})_{12}](\text{ClO}_4)_{16}$, was reported in the original communication^{10a} but we have collected another data set which has slightly increased the precision of the structure. It has the same arrangement of anions in and around the central cavity as does $[\text{Co}_8(\text{L}^{26\text{Py}})_{12}](\text{BF}_4)_{16}$, with one in the center and one sitting in the gap above the center of each of the six faces of the cube. The Zn···Zn separations are in the range 9.63 to 10.18 Å, with Zn(2) and Zn(2A) being the ions with a *fac* tris chelate arrangement, such that the Zn(2)—Zn(2A) vector is the *pseudo-C*₃ and *S*₆ axis.

(12) Hunter, C. A.; Sanders, J. K. M. *J. Am. Chem. Soc.* **1990**, *112*, 5525.
 (13) Claessens, C. G.; Stoddart, J. F. *J. Phys. Org. Chem.* **1997**, *10*, 254.

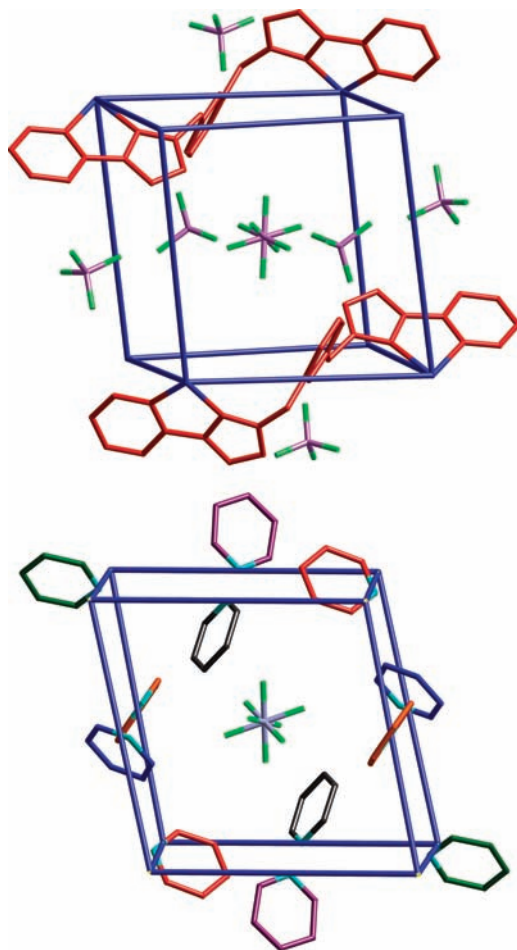


Figure 4. Two views of the structure of the complex cation of $[\text{Co}_8(\text{L}^{26\text{Py}})_{12}](\text{BF}_4)_{16}$. Top: a view showing only 2 of the 12 bridging ligands, emphasizing the presence of 1 anion in the center of the cavity (disordered over two sites, hence 8 apparent F positions with 50% occupancy), and an additional 6 located one over each face of the cube. Bottom: a view showing the orientation of the 12 pyridyl groups that are located on the edges of the cube (the N atoms are colored cyan to make their orientation clear).

Structures of Cross-Linked Double Helicates with Ni(II) and Co(II). Reaction of $\text{L}^{26\text{Py}}$ with $\text{Ni}(\text{BF}_4)_2$ afforded, after recrystallization, crystals of a complex $[\text{Ni}_4(\text{L}^{26\text{Py}})_6](\text{BF}_4)_8$ with a structure quite different from those above, and indeed hitherto unobserved in this series. It consists of two $\{\text{Ni}_2(\text{L}^{26\text{Py}})_2\}^{4+}$ double helical units of the same chirality, cross-linked by two additional $\text{L}^{26\text{Py}}$ ligands. The result (Figure 5) is an approximately square array of four Ni(II) ions, with $\text{Ni}\cdots\text{Ni}$ separations along the edge of between 10.01 and 10.17 Å. Two of the edges of the square are spanned by a pair of (crystallographically equivalent) ligands twisted into a double helical array; the other two are spanned by a single bridging ligand. The result is that each metal ion is coordinated by three bidentate fragments by different ligands, and the 2:3 metal/ligand ratio is maintained albeit in an unexpected structural type. As usual, on those edges spanned by a single bridging ligand, the central aromatic spacer of the ligand (here, the pyridine-2,6-diyl group) is sandwiched between two coordinated pyrazolylpyridine fragments from different ligands resulting in a three-component π -stacked sequence. All six

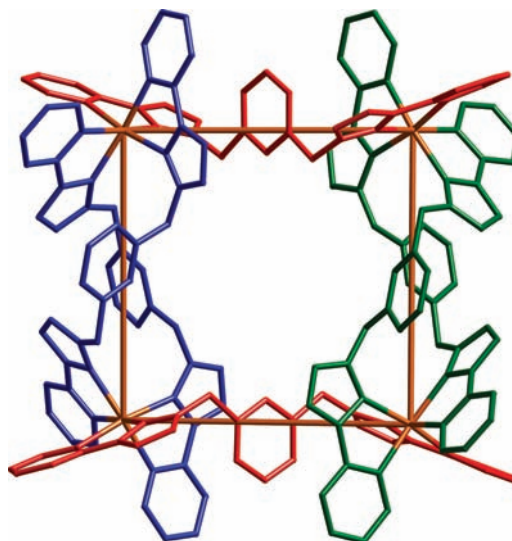


Figure 5. View of the complex cation of $[\text{Ni}_4(\text{L}^{26\text{Py}})_6](\text{BF}_4)_8$ with crystallographically equivalent ligands colored the same.

pyridine-2,6-diyl groups are oriented such that the N atoms are directed toward the center of the resulting cavity, and the cavity contains a region of electron density which was best modeled as the oxygen atom of a water molecule disordered over two closely spaced sites. The distance of these partial O atoms from the inwardly directed pyridyl N atoms (>4 Å) is too great for there to be any significant $\text{N}\cdots\text{HOH}$ hydrogen bonding. Given that we had to use the “SQUEEZE” command in PLATON to eliminate areas of diffuse electron density associated with extensively disordered solvent molecules, it is possible that these pyridyl N atoms may be interacting with disordered solvent molecules that could not however be located in the refinement.

The obvious question is why this structure should form in preference to an octanuclear cubic cage. As pointed out earlier the main structural difference between octahedral Co(II) or Zn(II) on the one hand, and octahedral Ni(II) on the other, is the lower ionic radius of Ni(II). In the structure of $[\text{Ni}_4(\text{L}^{26\text{Py}})_6](\text{BF}_4)_8$ the Ni–N distances lie in the range 2.09–2.14 Å with an average of 2.11 Å. In the cubic cage $[\text{Zn}_8(\text{L}^{26\text{Py}})_{12}](\text{ClO}_4)_{16}$, for example, the Zn–N distances span the range 2.13–2.27 Å with an average of 2.17 Å, and in $[\text{Co}_8(\text{L}^{13\text{Ph}})_{12}](\text{BF}_4)_{16}$ the Co–N distances span the range 2.12 to 2.20 Å with an average value of 2.15 Å. It appears, as we have noticed before, that the more compact coordination sphere around Ni(II) is just sufficient to prevent formation of the crowded cage structure in which ligands would be forced into uncomfortable proximity to one another. A related structural type, a square M_4L_6 assembly with the same arrangement of metal ions and ligands, has been prepared recently by Steel and co-workers.¹⁴

We expected the reaction of $\text{L}^{13\text{Ph}}$ with $\text{Co}(\text{ClO}_4)_2$ to generate an octanuclear cube with the same type of structure as the five examples reported earlier. However, uniquely in this series, this particular combination of metal ion, ligand, and counterion afforded crystals of a quite different structural type: the hexanuclear complex

(14) Steel, P. J. personal communication.

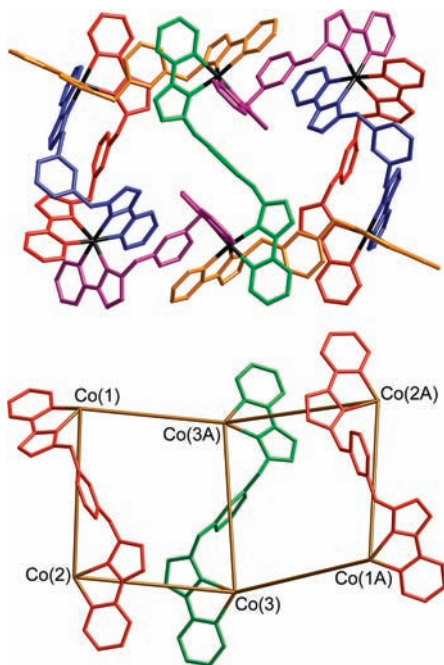


Figure 6. Two views of the structure of the metal complex framework of $[\text{Co}_6(\text{L}^{13\text{Ph}})_9][\text{ClO}_4]_{12}$ (only one independent complex unit is shown). Top: the whole metal–ligand assembly, with symmetry-equivalent ligands colored the same (note that there is a C_2 axis through the center of the green ligand such that there are 4.5 independent ligand environments, cf. Figure 11). Bottom: the “open-book” array of metal ions, and three of the edge-bridging ligands. Crystallographically equivalent ligands are colored the same in each case.

whose structure is shown in Figure 6.^{10b} This structure has no precedent that we are aware of in the literature. It consists of an unusual open framework structure based on an array of six Co(II) centers consisting of two squares that share an edge. The array is folded about the central two Co(II) ions, like an open book that is slightly folded along its spine, with a Co(II) ion at each corner and two defining the central spine. The 2:3 metal/ligand ratio requires nine ligands; there are two spanning each of the terminal pairs of Co(II) ions (the opposed open edges of the book, red and blue ligands in the figure) in a double helical arrangement, with all remaining Co–Co vectors (from each corner of the book to the spine, and along the central spine) having one bridging ligand. The two double helical sections are homochiral as they are related by a C_2 rotation through the center of the complex. The $\text{Co}\cdots\text{Co}$ separations lie in the range 9.66–9.97 Å (average 9.79 Å), with the Co–Co–Co angle at the spine (i.e., the extent of folding) being 119°. Co(2) and Co(3) have the same optical configuration as each other, and a *fac* tris-chelate geometry, with Co(1) having the opposite optical configuration and a *mer* tris-chelate geometry. There are numerous regions of aromatic π -stacking between near-parallel, overlapping sections of different ligands (e.g., red/orange/green, purple/green/purple, and blue/purple/yellow triple stacks, and red/blue and blue/purple stacks between pairs of ligand sections, using the color scheme in Figure 6).

This structure is conceptually related to that of the previous structure $[\text{Ni}_4(\text{L}^{26\text{Py}})_6](\text{BF}_4)_4$ in the way shown in Figure 7. In each case there is a pair of $\{\text{M}_2\text{L}_2\}$ double helical dinuclear units which constitute the ends of a pair

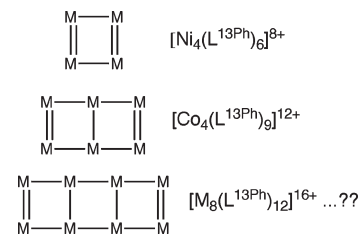


Figure 7. Sketch showing the structural relationship between the complexes $[\text{Ni}_4(\text{L}^{26\text{Py}})_6](\text{BF}_4)_8$ and $[\text{Co}_6(\text{L}^{13\text{Ph}})_9][\text{ClO}_4]_{12}$ (each solid line represents a bridging ligand) and the possibility of more extended members of the same series.

of parallel lines of metal ions which form a rectangular array. Every other adjacent pair of metal ions needs only one bridging ligand spanning them to give a connectivity of three at each metal center (i.e., three different ligands presenting three bidentate sites to the octahedral metal ions), but the terminal pairs of metal ions need to have two bridging ligands to close off the structure and provide coordinative saturation. One can imagine a potentially infinite sequence of such structures, all with a $2\text{M}/3\text{L}$ ratio, of which $[\text{Ni}_4(\text{L}^{26\text{Py}})_6](\text{BF}_4)_8$ and $[\text{Co}_6(\text{L}^{13\text{Ph}})_9](\text{ClO}_4)_{12}$ form the first two members (Figure 7). From a purely structural point of view these two complexes therefore are members of an interesting sequence that is quite different from the three-dimensional polyhedral cages such as the cubes described in the first section, but which are based on the same stoichiometric principles.

Solution Studies: Electrospray (ES) Mass Spectra and NMR Spectra. In this area of chemistry, crystallography alone, while of obvious value, does not give the whole picture, and it is necessary to examine the solution behavior of the compounds to see to what extent the solid state structure is maintained, or whether other species may form, in solution.

Starting with the simplest complex $[\text{Ni}_4(\text{L}^{26\text{Py}})_6](\text{BF}_4)_8$, the ES mass spectrum of redissolved crystals shows a sequence of peaks at m/z 1558, 1010, 736, and 571 that corresponds to the sequence of ions $\{\text{Ni}_4(\text{L}^{26\text{Py}})_6(\text{BF}_4)_{8-n}\}^{n+}$ ($n = 2, 3, 4, 5$) by successive loss of tetrafluoroborate ions. In every case the spacing between the component peaks of the isotope cluster was $1/n$, confirming that these peaks do arise from the intact tetranuclear complex and not from other metal/ligand combinations with different charges. [For example an m/z value of 736 could arise from a dinuclear species $\{\text{Ni}_2(\text{L}^{26\text{Py}})_3(\text{BF}_4)_2\}^{2+}$, or from an intact cube $\{\text{Ni}_8(\text{L}^{26\text{Py}})_{12}(\text{BF}_4)_8\}^{8+}$, but in these cases the isotope spacing would be $1/2$ or $1/8$, respectively, not $1/4$.] In addition the isotope pattern is in each case consistent with the presence of four Ni atoms. There is clear evidence of fragmentation under the conditions in the spectrometer, with numerous peaks for smaller species such as $\{\text{Ni}(\text{L}^{26\text{Py}})_3\}^{2+}$ (at $m/z = 619$) and $\{\text{Ni}_2(\text{L}^{26\text{Py}})_2(\text{BF}_4)_2\}^{2+}$ (at m/z 538), plus many others which could not be readily assigned, but it is clear that (i) there is a characteristic sequence of peaks corresponding to the intact tetranuclear cation $\{\text{Ni}_4(\text{L}^{26\text{Py}})_6\}^{8+}$ associated with varying numbers of cations, and (ii) no obvious evidence for formation of larger assemblies such as an octanuclear cube which give quite obvious sequences of peaks. The ESMS spectrum is therefore consistent with the solid state structure being retained in solution.

The behavior of the M_8L_{12} cube complexes in solution is less straightforward, something which is hinted at by our observation from the crystal structures that the same metal and ligand combination [$Co(II)$ with L^{13Ph}] can give crystals of either the octanuclear cube [$Co_8(L^{13Ph})_{12}(BF_4)_{16}$] (Figures 1, 2) or the hexanuclear “open book” structure [$Co_6(L^{13Ph})_9(ClO_4)_{12}$] (Figure 6). Since there is no obvious templating effect associated with the anions which would drive the assembly in one direction or the other, the conclusion from this is that two very similar energy assemblies can form and which one crystallizes is a matter of chance and the kinetics of crystallization. We might therefore expect to see both types of complex occurring in solution, and possibly even interconversion between them if they are labile enough.

$[Co_8(L^{26py})_{12}(BF_4)_{16}]$ presents straightforward behavior, showing in its ES mass spectrum a series of peaks for the intact cube with no evidence for any rearrangement to the “open book” form. The series of peaks was observed at m/z 2106, 1558, 1229, 1010, 853, 736, and 644, corresponding to the series $\{Co_8(L^{26py})_{12}(BF_4)_{16-n}\}^{n+}$ ($n = 3, 4, 5, 6, 7, 8, 9$, respectively) of intact octanuclear cubic cations associated with varying numbers of anions (Figure 8). Within this m/z range the peaks that would occur for the $\{Co_6(L^{26py})_9(BF_4)_{12-n}\}^{n+}$ series are completely absent.

In contrast, $[Co_8(L^{13Ph})_{12}(BF_4)_{16}]$ showed more complex solution behavior. This is the metal/ligand combination that yielded both types of crystal structure (albeit with different counterions: the tetrafluoroborate salt crystallizes the cube, but the perchlorate salt as the “open book”). Redissolved crystals of this cube complex afford the ES mass spectrum shown in Figure 9 which clearly contains two overlapping series of peaks. One series has peaks at m/z 2103, 1555, 1227, 108, 852, 734, which correspond to the intact cube cation associated with different numbers of tetrafluoroborate anions, namely, $\{Co_8(L^{13Ph})_{12}(BF_4)_{16-n}\}^{n+}$ ($n = 3, 4, 5, 6, 7, 8$, respectively). The other series has peaks at m/z 2375, 1555, 1145, 899, 734, and 618 which correspond to the hexanuclear “open book” complex $\{Co_6(L^{13Ph})_9(BF_4)_{12-n}\}^{n+}$ ($n = 2, 3, 4, 5, 6, 7$ respectively). The peaks at m/z 1555 and 734 are common to both: for example m/z 1555 can arise from both $\{Co_8(L^{13Ph})_{12}(BF_4)_{12}\}^{4+}$, and $\{Co_6(L^{13Ph})_9(BF_4)_9\}^{3+}$, but there are enough unique members of both series present for it to be quite clear that the crystals of $[Co_8(L^{13Ph})_{12}(BF_4)_{16}]$ have partially rearranged on dissolution to generate some $[Co_6(L^{13Ph})_9(BF_4)_{12}]$. Assuming that the intensities of the peaks in the different series relate to their respective concentrations, it is also clear that the cube is the major component, and the “open book” complex is the minor component.

Quite similar behavior was observed for $[Zn_8(L^{26py})_{12}(ClO_4)_{16}]$. The ES mass spectrum of redissolved crystals showed peaks at m/z 877 and 755, associated with the intact cube species $\{Zn_8(L^{26py})_{12}(ClO_4)_{16-n}\}^{n+}$ ($n = 7, 8$) and very weak peaks at m/z 1609 and 924, ascribable to the hexanuclear “open book” complex $\{Zn_6(L^{26py})_9(ClO_4)_{12-n}\}^{n+}$ ($n = 3, 5$). By far the most intense peak, however, was at m/z 556 with an isotope pattern consistent with the presence of one Zn atom; this corresponds to the mononuclear fragment $\{Zn(L^{26py})(ClO_4)\}^+$. The intensity of this, the relative weakness of the signals

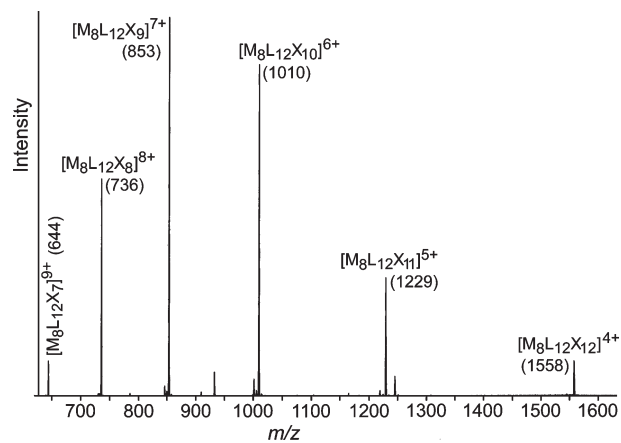


Figure 8. Part of the ES mass spectrum of $[Co_8(L^{26py})_{12}(BF_4)_{16}]$ in $MeNO_2$ showing a sequence of peaks for the intact cubic complex cation. $M = Co$, $L = L^{26py}$, $X = BF_4$.

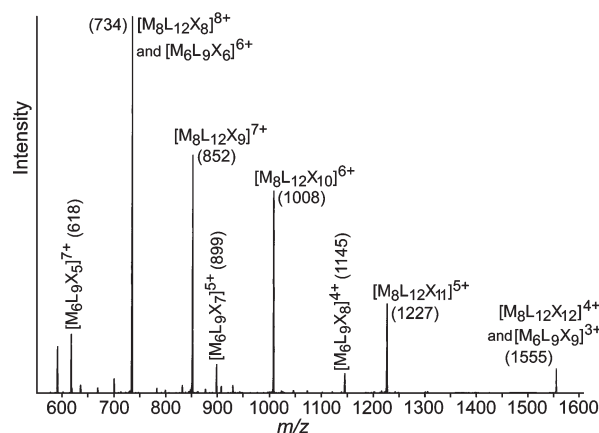


Figure 9. Part of the ES mass spectrum of $[Co_8(L^{13Ph})_{12}(BF_4)_{16}]$ in $MeNO_2$ showing sequences of peaks for both the intact cubic complex cation (more intense component) and the hexanuclear “open book” form (less intense component). $M = Co$, $L = L^{13Ph}$, $X = BF_4$.

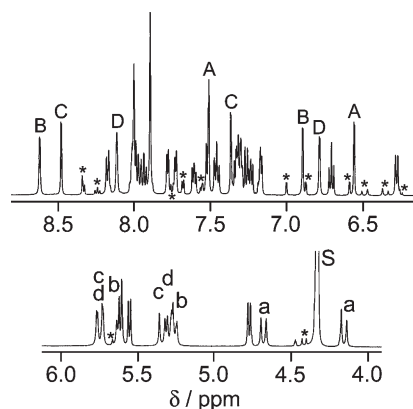


Figure 10. 1H NMR spectrum of $[Zn_8(L^{26py})_{12}(ClO_4)_{16}]$ (400 MHz, CD_3NO_2). The major peaks integrate to 38H as required for two independent ligand environments. Signals labeled a, b, c, d are the four pairs of doublets associated with the four independent diastereotopic methylene groups. Signals labeled A, B, C, D are the four pairs of doublets associated with the four independent pyrazolyl rings. Small signals marked * are due to a minor component associated with some rearrangement or dissociation in solution.

from the intact cube, and the presence of very weak signals from the “open book” form, all suggest that the

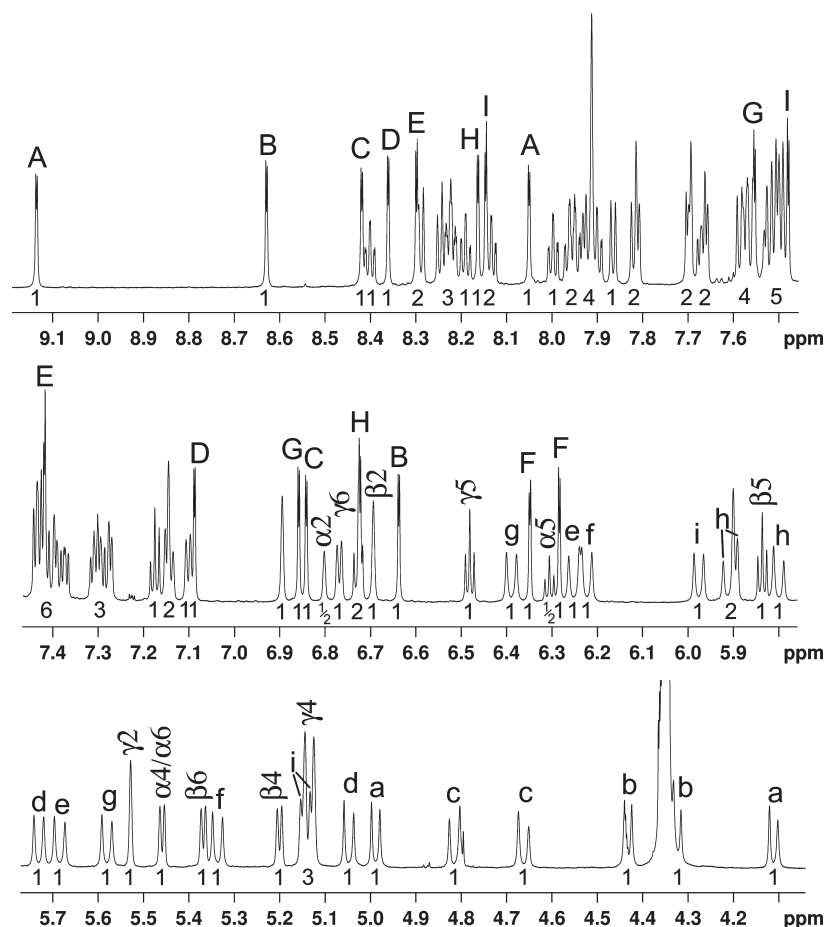


Figure 11. ^1H NMR spectrum (800 MHz, CD_3NO_2) of redissolved crystals $[\text{Zn}_8(\text{L}^{13\text{Ph}})_{12}](\text{ClO}_4)_{16}$ showing quantitative rearrangement to the hexanuclear “open book” form integrating to 90H (cf. Figure 6). Lower-case labels *a–i* denote the nine pairs of doublets associated with the nine independent diastereotopic methylene groups. Upper-case labels A–I denote the nine pairs of doublets associated with the nine independent pyrazolyl rings. Greek labels denote partial assignments of protons on the central 1,3-disubstituted phenylene rings (α , β , γ , etc.); note that $\alpha 2$ and $\alpha 5$ are half intensity as they alone lie on the 2-fold symmetry axis (cf. Figure 6, and see main text).

cube complex cation does not remain fully intact in solution.

The ^1H NMR spectrum of $[\text{Zn}_8(\text{L}^{26\text{py}})_{12}](\text{ClO}_4)_{16}$ confirms this (Figure 10). It does clearly show a major set of peaks consistent with the intact cube, comprising 38 independent proton environments from two independent ligands with no internal symmetry. One ligand type spans *fac* and *mer* metal centers, and the other spans two *mer* metal centers but with no internal symmetry because of the local chirality (Figure 2). There are six of each type of ligand in the complex, hence our observation of 38 independent proton environments of the same intensity. This is exactly what we have observed before in $\{\text{M}_8\text{L}_{12}\}$ cube cages with this same mixture of *fac* and *mer* tris-chelate metal centers leading to overall S_6 symmetry.¹¹ Although not all of the signals can be individually resolved and assigned, even using a 500 MHz spectrum, there is enough information to confirm the symmetry. In the low chemical shift region, 4–6 ppm, there are four pairs of doublets arising from the diastereotopic methylene groups, assigned on the basis of a COSY spectrum; these are labeled *a–d* in Figure 10. Similarly in the higher chemical shift region of 6–9 ppm there are four pairs of doublets associated with four inequivalent pyrazolyl rings (labeled A–D). There are also present numerous low-intensity peaks (ca. 20% relative intensity compared to

the major peaks, labeled * in the figure) which we ascribe to the presence of smaller fragments following some dissociation or rearrangement as was evident from the ES mass spectrum. The spectrum does however confirm that the cube is still the major component in solution.

The most surprising solution behavior of the cube complexes is exhibited by $[\text{Zn}_8(\text{L}^{13\text{Ph}})_{12}](\text{ClO}_4)_{16}$. If this structure were retained in solution we would expect to see signals from two independent ligand environments, as explained above, that is, 40 proton environments for two $\text{L}^{13\text{Ph}}$. Dissolution of this complex in CH_3NO_2 reveals in a clean ^1H NMR spectrum of much higher complexity than this (Figure 11): integration of the signals, taking the obvious isolated signals as 1H each, adds up to a total of 90 proton environments. This is clearly inconsistent with the structure of an intact cube. It is, however, exactly consistent with complete conversion of the cubic complex to the “open book” hexanuclear form in solution, with 4.5 independent ligand environments (four ligands having no internal symmetry, and a fifth having 2-fold symmetry). This can be related to the crystal structure shown in Figure 6a where the central ligand colored green lies on the C_2 axis.

The complexity of the spectrum is such that we needed a high field (800 MHz) ^1H NMR spectrum and COSY spectrum to facilitate analysis. In addition to the number

of signals observed, two features of this spectrum are particularly diagnostic and easy to see. First, we can locate via the COSY spectrum 18 methylene protons which are coupled in pairs because of the presence of nine inequivalent CH_2 groups, all of which are diastereotopic and generate a coupled pair of doublets. In the same way we can identify nine pairs of protons associated with the pyrazolyl rings. These are labeled on Figure 11. Second, there are two, and only two, half-intensity signals at 6.80 and 6.30 ppm, a singlet and triplet, respectively, which correspond to protons H^2 and H^5 of the central phenyl ring of the ligand that lies on the 2-fold axis. These are labeled $\alpha 2$ and $\alpha 5$ on Figure 11. As these are the only two protons in the structure that are on the 2-fold axis they will have half the intensity of all other signals which arise from a pair of equivalent protons. Thus, of the 180 protons in the complex (nine ligands containing 20 protons each), there are 89 pairs and two unique protons. The COSY spectrum confirms that these two protons are on the same aromatic ring as they both show couplings to the doublets for the pair of equivalent protons H^4 and H^6 (labeled as $\alpha 4/\alpha 6$, at 5.47 ppm). We conclude that crystals of the cube $[\text{Zn}_8(\text{L}^{13\text{Ph}})_{12}](\text{ClO}_4)_{16}$ rearrange quantitatively to the “open book” form on dissolution in MeNO_2 , which may explain why they were so slow to dissolve. The ES mass spectrum, even at low cone voltages, showed only peaks due to small fragments, principally m/z 947 for $\{\text{Zn}(\text{L}^{13\text{Ph}})_2(\text{ClO}_4)\}^+$, 753 for $\{\text{Zn}_2(\text{L}^{13\text{Ph}})_3(\text{ClO}_4)_2\}^{2+}$, 620 for $\{\text{Zn}(\text{L}^{13\text{Ph}})_3\}^{2+}$, and 424 for $\{\text{Zn}(\text{L}^{13\text{Ph}})_2\}^{2+}$. It was not possible in this case to detect the intact “open book” complex in solution although the ^1H NMR spectrum leaves no doubt that this is the form adopted by the complex in MeNO_2 solution.

Finally, we looked at the solution behavior of $[\text{Co}_6(\text{L}^{13\text{Ph}})_9](\text{ClO}_4)_{12}$, the only example that crystallized in the “open book” form. The peaks in the ^1H NMR spectrum (Figure 12) span the range -90 to $+116$ ppm because of the paramagnetism of the high-spin $\text{Co}(\text{II})$ centers. This spreads the peaks out nicely, and we and others have been able to use ^1H NMR spectroscopy of high-spin $\text{Co}(\text{II})$ complexes as a very useful diagnostic technique.^{8c,11,15} The intensity and width of the peaks varies substantially, as is always the case: peak width is inversely proportional to T_1 for each proton, which in turn is related to the sixth power of the distance of the relevant proton from the paramagnetic $\text{Co}(\text{II})$ centers. In this spectrum we can identify 81 distinct signals (labeled with asterisks in Figure 12). This is clearly inconsistent with the existence of a cubic complex in solution (which would give 40 proton environments) but is quite consistent with the structure of the “open book” being retained which would afford 90 proton environments. Of the missing 9 signals some will be obscured by the intense solvent/water peaks in the 0–5 ppm range, and some are presumably too broad and weak to see. The ^1H NMR spectrum suggests therefore that the “open book” crystals retain their structure in solution with no rearrangement to

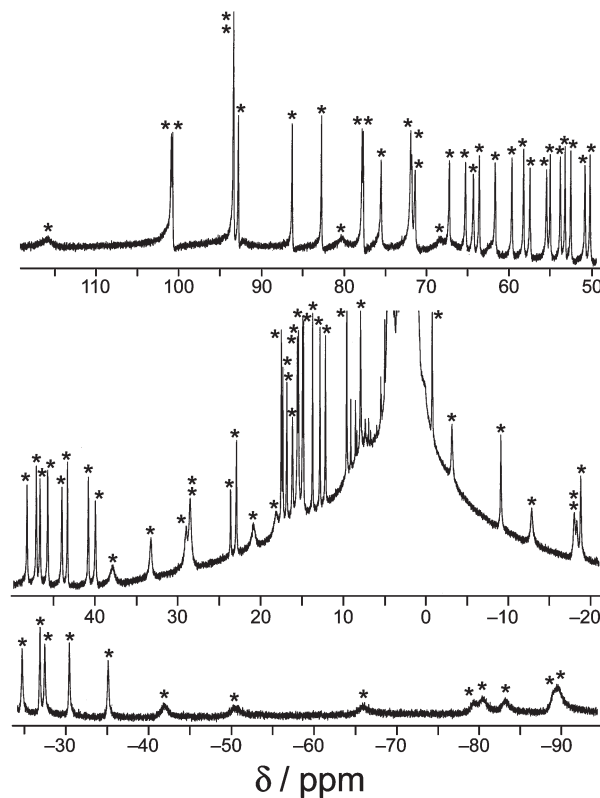


Figure 12. ^1H NMR spectrum (400 MHz, CD_3NO_2) of redissolved crystals of $[\text{Co}_6(\text{L}^{13\text{Ph}})_9](\text{ClO}_4)_{12}$ whose paramagnetism has spread the peaks out over a range of about 200 ppm. Signals that can be clearly identified are denoted by an asterisk, *; 81 of the expected 90 signals can be located.

form the cube. ESMS indirectly confirms this, as we could not identify any peaks that would be expected for an octanuclear cube complex. The spectrum did, however, show weak peaks at m/z 1594 and 1170 ascribable to $\{\text{Co}_6(\text{L}^{13\text{Ph}})_9(\text{ClO}_4)_{12-n}\}^{n+}$ ($n = 3, 4$) as well as numerous more intense peaks at lower m/z values because of smaller fragments.

Conclusions

The combination of X-ray crystallographic, ^1H NMR, and ESMS studies reveal interesting behavior for these complexes. The tetranuclear square complex $[\text{Ni}_4(\text{L}^{26\text{Py}})_6](\text{BF}_4)_8$, while structurally interesting in that it contains two cross-linked double helicates, is straightforward in that there is no evidence for formation of other species. Similarly, the structurally related complex $[\text{Co}_6(\text{L}^{13\text{Ph}})_9](\text{ClO}_4)_{12}$, which adopts the “open book” structure with two double helical dinuclear units at the ends, retains its structure in solution as shown by both ^1H NMR and ESMS studies.

The remaining $\text{Co}(\text{II})$ and $\text{Zn}(\text{II})$ complexes with either $\text{L}^{26\text{py}}$ or $\text{L}^{13\text{Ph}}$ crystallize as the octanuclear cubes $[\text{M}_8\text{L}_{12}]\text{X}_{16}$, all with the same basic structural type in which a mixture of *fac* and *mer* tris-chelate metal centers results in pseudo- S_6 symmetry. The large central cavities contain varying numbers of counterions (1, 2, or 4). Despite the similarity in their solid state structures, their solution behavior, however, is highly variable. Some of them remain in solution either completely or nearly completely as the cubes: this behavior is shown by $[\text{Co}_8(\text{L}^{26\text{py}})_{12}](\text{BF}_4)_{16}$ (on the basis of ES mass spectrometry) and $[\text{Zn}_8(\text{L}^{26\text{py}})_{12}](\text{ClO}_4)_{16}$ (on the basis of ^1H NMR

(15) (a) Constable, E. C.; Martínez-Máñez, R.; Cargill Thompson, A. M. W.; Walker, J. V. *J. Chem. Soc., Dalton Trans.* **1994**, 1585. (b) Constable, E. C.; Daniels, M. A. M.; Drew, M. G. B.; Tocher, D. A.; Walker, J. V.; Wood, P. D. *J. Chem. Soc., Dalton Trans.* **1993**, 1947. (c) Amouri, H.; Mimassi, L.; Rager, M. N.; Mann, B. E.; Guyard-Duhayon, C.; Raehm, L. *Angew. Chem., Int. Ed.* **2005**, *44*, 4543.

Table 1. Crystal Parameters, Data Collection, and Refinement Details for the Structures in This Paper

complex	[Co ₈ (L ^{13Ph}) ₁₂]- (BF ₄) ₁₆ ·H ₂ O·(MeNO ₂) ₁₈	[Co ₈ (L ^{26Py}) ₁₂]- (BF ₄) ₁₆	[Zn ₈ (L ^{26Py}) ₁₂]- (ClO ₄) ₁₆	[Zn ₈ (L ^{13Ph}) ₁₆]- (ClO ₄) ₁₆ ·(MeNO ₂) _{5.5} · (dmf) ₂ ·(H ₂ O) ₄	[Ni ₄ (L ^{26Py}) ₆]- (BF ₄) ₈ ·(H ₂ O) _{0.5}
formula	C ₃₀₆ H ₂₉₆ B ₁₆ ⁻ Co ₈ F ₆₄ N ₉₀ O ₃₇	C ₂₇₆ H ₂₂₈ B ₁₆ ⁻ Co ₈ F ₆₄ N ₈₄	C ₂₇₆ H ₂₂₈ Cl ₁₆ ⁻ N ₈₄ O ₆₄ Zn ₈	C _{299.5} H _{278.5} ⁻ Cl ₁₆ N _{79.5} O ₈₁ Zn ₈	C ₁₃₈ H ₁₁₅ B ₈ F ₃₂ ⁻ N ₄₂ Ni ₄ O _{0.5}
molecular weight	7686.73	6581.82	6835.58	7377.68	3299.04
T, K	150(2)	150(2)	150(2)	150(2)	150(2)
crystal system	triclinic	monoclinic	triclinic	triclinic	monoclinic
space group	P1	P2(1)/c	P1	P1	C2/c
a, Å	22.870(3)	19.5900(9)	23.040(6)	20.9658(10)	21.3802(15)
b, Å	23.585(3)	42.658(2)	23.307(6)	21.8992(10)	19.4021(15)
c, Å	25.043(3)	21.1943(9)	26.686(6)	21.9285(11)	37.083(3)
α, deg	113.727(6)	90	65.408(6)	60.570(3)	90
β, deg	109.603(7)	113.099(2)	89.833(6)	78.875(3)	103.357(3)
γ, deg	101.195(6)	90	61.512(5)	89.377(3)	90
V, Å ³	10768(3)	16291.6(13)	11104(5)	8562.5(7)	14966.7(19)
Z	1	2	1	1	4
ρ, g cm ⁻³	1.185	1.342	1.022	1.431	1.464
crystal size, mm ³	0.3 × 0.3 × 0.2	0.2 × 0.2 × 0.2	0.4 × 0.4 × 0.4	0.2 × 0.2 × 0.05	0.4 × 0.4 × 0.4
μ, mm ⁻¹	0.391	0.497	0.583	0.765	0.601
data, restraints, parameters	48594, 337, 2242	21281/497/2089	28016, 2461, 1637	29091, 437, 2187	17195, 245, 1003
final R1, wR2 ^a	0.1153, 0.3556	0.0985, 0.2897	0.1523, 0.4267	0.0894, 0.2950	0.1346, 0.3765

^a The value of R1 is based on "observed" data with $I > 2\sigma(I)$; the value of wR2 is based on all data.

which shows the cube to be the dominant species in solution). Some of the cube complexes show clear evidence for *partial* conversion to an "open book" structure in solution: this is shown most clearly for [Co₈(L^{13Ph})₁₂](BF₄)₁₆ whose ES mass spectrum shows sequences of peaks for both cube and "open book" species. One of the cube complexes, [Zn₈(L^{13Ph})₁₂](ClO₄)₁₆, remarkably, converts *completely* to the open-book form on dissolution as shown by the ¹H NMR spectrum.

These differences are difficult to rationalize beyond the fairly obvious statement that the two types of structure must be similar in energy, and small differences in factors such as solubility and metal-based stereoelectronic preferences [absent for Zn(II) but not for Co(II)] must play significant roles in deciding which structure dominates; the results are, however, quite clear.

Experimental Section

General Details. The ligands L^{26Py} and L^{13Ph} were prepared as reported previously.¹⁰ Electrospray mass spectra were recorded using a low cone voltage (typically 5 V) on a Micromass LCT instrument. ¹H NMR spectra were recorded on Bruker Avance-2 400, DRX-500, or DRX-800 instruments.

Complex Syntheses: Solvothermal Method. This method was used for all tetrafluoroborate salts. A Teflon-lined autoclave was charged with the appropriate M(BF₄)₂ salt (0.085 mmol, ca. 29 mg depending on the metal), either L^{13Ph} or L^{26Py} (0.13 mmol, ca. 50 mg depending on the ligand), and methanol (9 cm³). The mixture was heated to 100 °C for 12 h and then cooled slowly to room temperature to yield crystals of the product in good yield (80–90%). In most cases these were of X-ray quality and could be examined directly; in some cases the crystals obtained in this way were too small for X-ray analysis so were recrystallized from nitromethane/ether. The vacuum-dried samples were observed to be slightly hygroscopic, and elemental analyses were consistent in most cases with the presence of several molecules of water per complex formula unit. Analytical data are as follows. Mass spectroscopic data are discussed in the main text.

[Ni₄(L^{26Py})₆](BF₄)₈ (purple crystals). Found: C, 49.2; H, 3.5; N, 17.3%. Required for [Ni₄(L^{26Py})₆](BF₄)₈·5H₂O: C, 49.0; H, 3.7; N, 17.4%.

[Co₈(L^{26Py})₁₂](BF₄)₁₆ (orange crystals). Found: C, 48.7; H, 3.7; N, 16.8%. Required for [Co₈(L^{26Py})₁₂](BF₄)₁₆·12H₂O: C, 48.7; H, 3.7; N, 17.3%.

[Co₈(L^{13Ph})₁₂](BF₄)₁₆ (orange crystals). Found: C, 51.6; H, 3.9; N, 14.9%. Required for [Co₈(L^{13Ph})₁₂](BF₄)₁₆·7H₂O: Found: C, 51.7; H, 3.8; N, 15.0%.

Complex Syntheses: Room-Temperature Solution Method.

This method was used for all perchlorate salts, and the example given is representative. A solution of Zn(ClO₄)₂·6H₂O (0.032 g, 0.086 mmol) in MeOH (7 cm³) was added to a solution of L^{26Py} (0.05 g, 0.13 mmol) in CH₂Cl₂ (7 cm³). The mixture was stirred at room temperature for 24 h, and the resultant precipitate was filtered off, washed with both MeOH and CH₂Cl₂, and dried in vacuo to give [Zn₈(L^{26Py})₁₂](ClO₄)₁₆ as a colorless powder in 90% yield. X-ray quality crystals were grown by slow diffusion of diethyl ether into a solution of the complex in DMF or nitromethane.

[Zn₈(L^{26Py})₁₂](ClO₄)₁₆ (colorless crystals). Found: C, 48.5; H, 3.8; N, 17.0. Required: C, 48.5; H, 3.4; N, 17.2%.

[Zn₈(L^{13Ph})₁₆](ClO₄)₁₆ (colorless crystals). Found: C, 49.5; H, 3.5; N, 14.4. Required for [Zn₈(L^{13Ph})₁₆](ClO₄)₁₆·5H₂O: C, 50.0; H, 3.6; N, 14.6%.

X-ray Crystallography. Crystals were removed from the mother liquor, coated with oil, and transferred to a stream of cold N₂ on the diffractometer as quickly as possible to prevent decomposition because of solvent loss. All new structural determinations (i.e., not including those that were first reported in the earlier communications¹⁰) were carried out on a Bruker SMART-APEX2 diffractometer using graphite-monochromated Mo Kα radiation (λ = 0.71073 Å) from a sealed tube source.

Crystals of the metal complexes scattered relatively weakly because of the extensive disorder of anions and solvent molecules. After integration of the raw data, and before merging, an empirical absorption correction was applied (SADABS)¹⁶ based on comparison of multiple symmetry-equivalent measurements. The structures were solved by direct methods and refined by full-matrix least-squares on weighted F² values for all reflections using the SHELX suite of programs.¹⁷ Pertinent crystallographic data are collected in Table 1. In every case (i) the

(16) Sheldrick, G. M. *SADABS: A program for absorption correction with the Siemens SMART system*; University of Göttingen: Göttingen, Germany, 1996.

(17) Sheldrick, G. M. *Acta Crystallogr., Sect. A* **2008**, *64*, 112.

weakness of the data required extensive use of restraints and/or constraints, to keep the geometries of anions, aromatic rings, or solvent molecules reasonable; and (ii) there was disorder associated with anions and (where located) solvent molecules. In addition, in all cases except for $[\text{Zn}_8(\text{L}^{13\text{Ph}})_{16}](\text{ClO}_4)_{16} \cdot (\text{MeNO}_2)_{5.5} \cdot (\text{dmf})_2 \cdot (\text{H}_2\text{O})_4$, there were extensive areas of residual electron density which could not sensibly be modeled as solvent or anions, which were removed via application of the "Squeeze" function in PLATON.¹⁸ Full details of these issues and how they were handled is given in the individual CIFs in the Supporting Information.

(18) Spek, A. L. *J. Appl. Crystallogr.* **2003**, *36*, 7.

Acknowledgment. We thank Drs. Andrea Houslow and Brian Taylor for assistance with the NMR spectroscopy, Mr. Simon Thorpe and Mrs. Sharon Spey for assistance with the mass spectrometry, and the University of Garyounis in Libya for a Ph.D. studentship to Mr. Adel Najar. The contributions of Dr. Zöe Bell and Dr. Stephen Argent to the preliminary communications preceding this paper are also gratefully acknowledged.

Supporting Information Available: Crystallographic data in CIF format. This material is available free of charge via the Internet at <http://pubs.acs.org>.